Crystallization and preliminary X-ray diffraction characterization of the XccFimXEAL-c-di-GMP and XccFimXEAL-c-di-GMP-XccPilZ complexes from Xanthomonas campestris

Liao, Yi-Ting; Chin, Ko-Hsin; Kuo, Wei-Ting; Chuah, Mary Lay-Cheng; Liang, Zhao-Xun; Chou, Shan-Ho

Crystallization and preliminary X-ray diffraction characterization of the XccFimX^{EAL}–c-di-GMP and XccFimX^{EAL}–c-di-GMP–XccPilZ complexes from Xanthomonas campestris

Yi-Ting Liao,[a] Ko-Hsin Chin,[b] Wei-Ting Kuo,[a] Mary Lay-Cheng Chuah,[c] Zhao-Xun Liang[c] and Shan-Ho Chou[a,b,d]*

[a]Institute of Biochemistry, National Chung Hsing University, Taichung 40227, Taiwan, [b]Agricultural Biotechnology Center, National Chung Hsing University, Taichung 40227, Taiwan, [c]School of Biological Sciences, Nanyang Technological University, Singapore 637551, Singapore, and [d]Graduate Institute of Basic Medical Science, China Medical University, Taichung 40402, Taiwan

Correspondence e-mail: shchou@nchu.edu.tw

c-di-GMP is a major secondary-messenger molecule in regulation of bacterial pathogenesis. Therefore, the c-di-GMP-mediated signal transduction network is of considerable interest. The PilZ domain was the first c-di-GMP receptor to be predicted and identified. However, every PilZ domain binds c-di-GMP with a different binding affinity. Intriguingly, a noncanonical PilZ domain has recently been found to serve as a mediator to link FimX^{EAL} to the PilB or PilT ATPase to control the function of type IV pili (T4P). It is thus essential to determine the structure of the FimX^{EAL}–PilZ complex in order to determine how the binding of c-di-GMP to the FimX^{EAL} domain induces conformational change of the adjoining noncanonical PilZ domain, which may transmit information to PilB or PilT to control T4P function. Here, the preparation and preliminary X-ray diffraction studies of the XccFimX^{EAL}–c-di-GMP and XccFimX^{EAL}–c-di-GMP–XccPilZ complexes from Xcc (Xanthomonas campestris pv. campesteris) are reported. Detailed studies of these complexes may allow a more thorough understanding of how c-di-GMP transmits its effects through the degenerate EAL domain and the noncanonical PilZ domain.

1. Introduction

Cyclic di-GMP (c-di-GMP) was first identified as a positive allosteric effector of cellulose synthase in the bacterium *Acetobacter xylinum* more than 20 years ago (Ross *et al.*, 1987, 1990), but has recently emerged as an important secondary messenger that controls a variety of cellular activities, such as the biogenesis of biofilms, flagella and pili in diverse bacteria. These activities have been correlated with bacterial pathogenicity (Römling *et al.*, 2005; Jenal & Malone, 2006; Römling & Amikam, 2006). Diguanylate cyclases (DGCs) containing the GGDEF domain and phosphodiesterases (PDEs) containing the EAL domain (Tal *et al.*, 1988; Simm *et al.*, 2004; Tischler & Camilli, 2004; Römling *et al.*, 2005) or the HD-GYP domain (Slater *et al.*, 2000; Ryan *et al.*, 2006) are responsible for the synthesis and degradation of c-di-GMP, respectively. However, it is still unclear how many targets of c-di-GMP are available and how this important secondary messenger mediates signal transduction in the cell. The components and responses of c-di-GMP signalling pathways are hot topics that are still being actively pursued (Römling, 2011).

PilZ-domain-containing proteins were suggested to be c-di-GMP receptors by a bioinformatics study (Amikam & Galperin, 2006) and this was subsequently demonstrated to be the case by several biochemical and structural studies (Ryjenkov *et al.*, 2006; Merighi *et al.*, 2007; Pratt *et al.*, 2007; Ramelot *et al.*, 2007). However, two types of PilZ domains were soon discovered: a type I PilZ domain that contains conserved R*XXX*R and D/N*X*S*XX*G signature motifs in the N-terminal region and experiences considerable conformational changes upon c-di-GMP binding (Benach *et al.*, 2007), and a type II PilZ domain that lacks such signature motifs and is unable to bind c-di-GMP directly. PA2960 from *Pseudomonas aeruginosa* is possibly the best known type II protein and is the first PilZ domain (Alm *et al.*, 1996) known to be required for T4P-mediated twitching mobility (Mattick, 2002). In *Xanthomonas campestris* pv. *campesteris* (*Xcc*), four PilZ-domain proteins were discovered and were found to be essential for its pathogenicity (McCarthy *et al.*, 2008); two of them

crystallization communications

contain a regular type I sequence and the other two contain a type II noncanonical sequence. XCC_{1028} is one of the type II domain-containing proteins; it adopts a similar five-stranded β-barrel structure, yet exhibits considerable differences at the N-terminal end owing to a lack of the characteristic N-terminal c-di-GMP binding signature motifs (Li, Chin, Liu *et al.*, 2009). XCC_{6012} is another example; it adopts a monomer structure similar to that of XCC_{1028}, yet is interrupted in the middle by two extra long helices between the $\beta1$ and $\beta2$ strands and self-assembles into a tetramer *via* the extra $\alpha3$ heptad-repeat helix (Li *et al.*, 2011). How type II PilZ domains respond to the c-di-GMP signal remains unclear to date.

FimX is a large multi-domain protein containing a tandem of REC, PAS, GGDEF and EAL domains that governs bacterial twitching motility (Huang *et al.*, 2003; Kazmierczak *et al.*, 2006). Interestingly, the REC, GGDEF and EAL domains in FimX are all degenerate: the REC domain lacks the crucial Asp essential for phosphotransfer, the GGDEF domain contains a rather unusual GDSIF motif and the EAL domain contains a modified EVL motif at the active site. Several biochemical and structural analyses have revealed the role of the degenerate EAL domain as the high-affinity binding receptor of c-di-GMP (Navarro *et al.*, 2009; Qi *et al.*, 2011). The crystal structure of a degenerate EAL domain from *P. aeruginosa* has also been solved (Navarro *et al.*, 2009).

Recently, a detailed study of the interaction between the $FimX^{EAL}$ and PilZ domains from *Xac* (*X. axonopodis* pv. *citri*) has been carried out using a variety of techniques such as NMR, thermal melting, far-Western blotting and *in vivo* motility assay methods (Guzzo *et al.*, 2009). From these studies, it was concluded that *Xac*PilZ binds to the *Xac*PilB ATPase required for T4P polymerization and to the $XacFimX^{EAL}$ domain required for binding c-di-GMP to regulate T4P biogenesis. However, the crucial $FimX^{EAL}$−PilZ complex structure is not available to date. Since the sequence and structure of *Xac*PilZ were found to be identical to those of $XccPilZ_{1028}$ (Guzzo *et al.*, 2009; Li, Chin, Liu *et al.*, 2009), and the $FimX^{EAL}$ sequences from both *Xcc* and *Xac* align very well with an identity of 90.9% and a similarity of 93.3% (data not shown), a similar interaction between the $FimX^{EAL}$ and PilZ domains is very likely to exist in *Xcc*. Here, we report the expression, purification, crystallization and preliminary X-ray diffraction studies of the $XccFimX^{EAL}$–c-di-GMP and $XccFimX^{EAL}$–c-di-GMP–$XccPilZ_{1028}$ complexes from *Xcc*. This phytopathogen is ideal for studying c-di-GMP-related issues since it contains a considerable number of GGDEF-domain, EAL-domain, HD-GYP-domain and PilZ-domain proteins (Ryan *et al.*, 2007; McCarthy *et al.*, 2008). Detailed studies of the $XccFimX^{EAL}$–c-di-GMP and $XccFim$-$FimX^{EAL}$–c-di-GMP–$XccPilZ$ complexes may allow a more thorough understanding of how c-di-GMP transmits its effects through non-canonical PilZ-domain proteins.

2. Materials and methods

2.1. Reagents

c-di-GMP was produced by an enzymatic method using an altered thermophilic DGC enzyme as described previously (Rao *et al.*, 2009).

2.2. Cloning and purification

$XccFimX^{EAL}$ was PCR-amplified directly from the plant pathogen *X. campestris* pv. *campestris* strain 17 (*Xcc*) using the forward primer 5′-TACTTCCAATCCAATGCTGAGGAAGAACGCATCGAGCG-C-3′ and the reverse primer 5′-TTATCCACTTCCAATGCTAGTA-GTCGCCCGGCCACCCGCG-3′. The PCR fragment exhibited the correct size in an agarose-gel electrophoresis experiment and was

confirmed by DNA sequencing. A ligation-independent cloning (LIC) approach (Aslanidis & de Jong, 1990; Stols *et al.*, 2001; Wu *et al.*, 2005) was used to obtain the desired constructs. The final construct codes for an N-terminal His_6 tag, a 17-amino-acid linker and the $XccFimX^{EAL}$ target under the control of a T7 promoter. Over-expression of the His_6-tagged target protein was induced by the addition of 800 µl 500 m*M* IPTG to the medium solution (to give a final IPTG concentration of 0.5 m*M*) at 293 K for 18 h. The target protein was purified by immobilized metal-affinity chromatography (IMAC) on a nickel column (Sigma) equilibrated with a buffer consisting of 20 m*M* Tris–HCl pH 8.0, 80 m*M* NaCl. The target protein was eluted with a gradient of 50–300 m*M* imidazole in the same buffer. The fractions containing $XccFimX^{EAL}$ were monitored using 13% SDS–PAGE and recombined. The His_6 tag and linker were then cleaved from the $XccFimX^{EAL}$ target using TEV (tobacco etch virus) protease at 289 K for 10 h. For crystallization, the $XccFimX^{EAL}$ protein was further purified on a Sephadex gel-filtration column (ÄKTA, Pharmacia Inc.). The final target-protein sample exhibited a purity greater than 99% as revealed by SDS–PAGE gel analysis (Fig. 1). It contained only an extra tripeptide (SNA) from the vector at the N-terminal end. SeMet-labelled $XccFimX^{EAL}$ was prepared in a similar way, except that it was produced using a non-auxotroph *Escherichia coli* strain BL21 (DE3) as host in the absence of methionine but with ample amounts of SeMet (100 mg l^{-1}). The M9 medium consisted of 1 g ammonium chloride, 3 g KH_2PO_4, 6 g
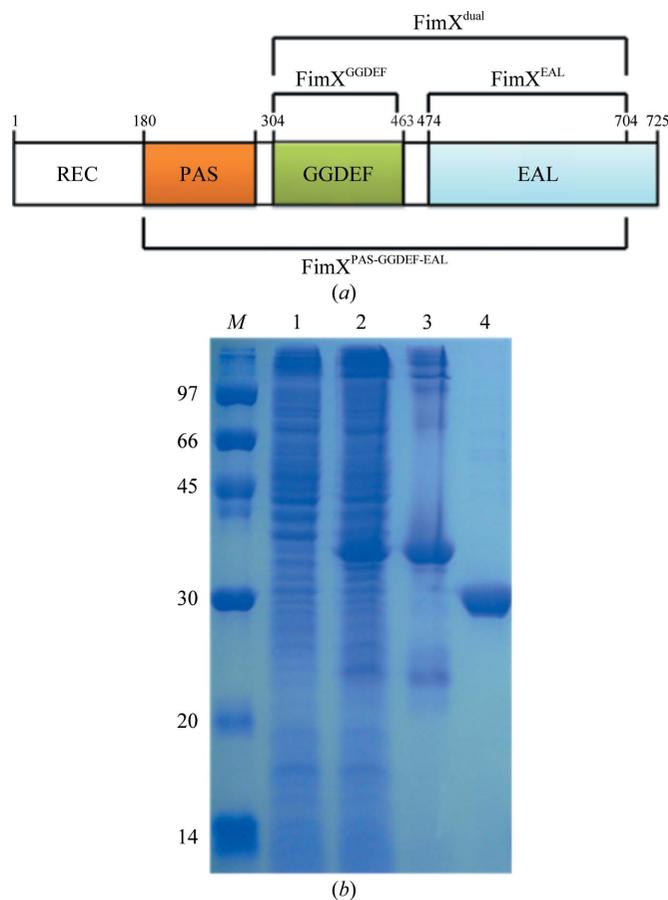

Figure 1
(*a*) The domain architecture and constructs used in these studies. (*b*) SDS–PAGE (13%) monitoring of the overexpression and purification of $XccFimX^{EAL}$. Lane 1, protein markers (labelled in kDa); lane 2, whole cell lysate before IPTG induction; lane 3, whole cell lysate after IPTG induction; lane 4, supernatant of His_6-tagged $XccFimX^{EAL}$; lane 5, gel-purified $XccFimX^{EAL}$ after TEV cleavage.

Table 1
Summary of the native and Se-SAD crystallographic data for the XccFimX^{EAL}–c-di-GMP and SeMet-XccFimX^{EAL}–c-di-GMP–XccPilZ$_{1028}$ complexes.

Values in parentheses are for the outermost shell.

	XccFimX^{EAL}–c-di-GMP	SeMet-XccFimX^{EAL}–c-di-GMP–XccPilZ$_{1028}$†
	Native	Peak
Beamline	NSRRC BL13B1	Spring-8
Wavelength (Å)	1.00000	0.97934
Space group	$P3_221$	$P6_322$
Unit-cell parameters (Å, °)	$a = b = 65.67$, $c = 121.29$, $\gamma = 120$	$a = b = 158.22$, $c = 64.81$, $\gamma = 120$
Resolution range (Å)	30–2.5 (2.59–2.50)	30–2.7 (2.80–2.70)
Total reflections	68379 (5890)	189837 (16170)
Unique reflections	19685 (1899)	49419 (4899)
Multiplicity	3.5 (3.1)	3.8 (3.3)
Completeness (%)	97.1 (93.5)	99.4 (98.7)
R_{merge}‡ (%)	3.6 (22.1)	13.8 (55.2)
$\langle I/\sigma(I)\rangle$	30.5 (5.4)	7.8 (1.8)
Matthews coefficient (Å^3 Da^{-1})	2.74	2.93
Solvent content (%)	55.2	58.0

† The FOM (figure of merit) for the SAD data for this complex was 0.37. ‡ $R_{merge} = \sum_{hkl} \sum_i |I_i(hkl) - \langle I(hkl)\rangle| / \sum_{hkl} \sum_i I_i(hkl)$, where $I_i(hkl)$ is the ith intensity measurement of reflection hkl, including symmetry-related reflections, and $\langle I(hkl)\rangle$ is its average.

Na$_2$HPO$_4$ supplemented with 20%(w/v) glucose, 0.3%(w/v) MgSO$_4$ and 10 mg FeSO$_4$ in 1 l double-distilled water. Induction was sustained at 293 K for 18 h by the addition of 0.45 ml 0.5 mM IPTG. The purification of the SeMet-labelled XccFimX^{EAL} protein was performed using the same procedure as for the native protein.

The XccPilZ$_{1028}$ sample was obtained using a similar protocol to that previously published (Li, Chin, Shih $et\ al.$, 2009).

2.3. Crystallization

For crystallization, the native XccFimX^{EAL} protein was concentrated to 0.56 mM in 20 mM Tris–HCl pH 8.0, 80 mM sodium chloride using an Amicon Ultra-10 (Millipore). The SeMet-XccFimX^{EAL}–XccPilZ$_{1028}$ complex (1:1 ratio) was concentrated to 0.075 mM in a similar way. Appropriate volumes of 25.6 mM c-di-GMP were added to the XccFimX^{EAL} and SeMet-XccFimX^{EAL}–XccPilZ$_{1028}$ complex solutions to prepare samples for cocrystallization with a 2:1 ligand: protein ratio. Screening for crystallization conditions for each protein was performed using sitting-drop vapour diffusion in 96-well plates (Hampton Research) at 277 K by mixing 0.5 µl protein solution with 0.5 µl reservoir solution and equilibrating against 50 µl reservoir solution. Initial screens including the sparse-matrix Crystal Screen and Crystal Screen 2 (Hampton Research), a systematic PEG–pH screen and the PEG/Ion screen (Hampton Research) were performed using a Gilson C240 crystallization workstation. Cubic crystals of the XccFimX^{EAL}–c-di-GMP complex appeared in 7 d from drops equilibrated against 50 µl reservoir solution comprising 20% PEG 3350, 0.2 M sodium formate pH 7.2, while hexagonal crystals of the SeMet-XccFimX^{EAL}–c-di-GMP–XccPilZ$_{1028}$ complex appeared in 21 d from drops equilibrated against 50 µl reservoir solution comprising 0.2 M NaCl, 0.1 M HEPES pH 7.5, 20% PEG 3K (Fig. 2). Crystals of both complexes suitable for diffraction experiments were grown from drops by mixing 1.5 µl protein solution with 1.5 µl reservoir solution and equilibrating against 500 µl reservoir solution at 277 K. Crystals of the XccFimX^{EAL}–c-di-GMP complex reached dimensions of 0.2 × 0.2 × 0.2 mm after one week, while those of the SeMet-XccFimX^{EAL}–c-di-GMP–XccPilZ$_{1028}$ complex reached dimensions of 0.01 × 0.01 × 0.01 mm after three weeks.

2.4. Data collection and processing

Crystals of both complexes were flash-cooled at 100 K under a stream of cold nitrogen gas using the reservoir solution as cryoprotectant. Before data collection, the crystals were scanned for Se absorption and 0.97934 Å was found to be the peak wavelength of the anomalous signal. X-ray diffraction data for the native XccFimX^{EAL}–c-di-GMP complex were obtained to 2.5 Å resolution on beamline 13B1 at the National Synchrotron Radiation Research Center (NSRRC), Taiwan, while those for the SeMet-XccFimX^{EAL}–c-di-GMP–XccPilZ$_{1028}$ complex were collected to 2.7 Å resolution on beamline 12B2 at SPring-8, Japan (Fig. 3). The data were indexed and integrated using the HKL-2000 processing software (Otwinowski & Minor, 1997), generating data sets that were 97.1 and 99.4% complete with an overall R_{merge} of 3.6 and 13.8% on intensities, respectively. Determination and refinement of the selenium positions, phase calculation and density modification were carried out using the programs $SOLVE$ and $RESOLVE$ (Terwilliger & Berendzen, 1999). Molecular replacement was performed using CNS (Brünger $et\ al.$, 1998). The crystals of the XccFimX^{EAL}–c-di-GMP complex belonged
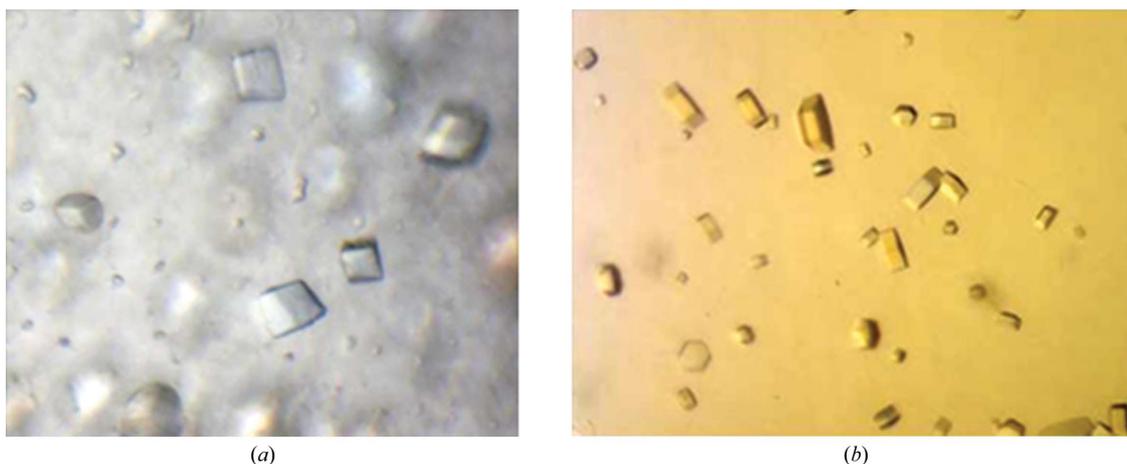

(a)

(b)

Figure 2
Crystals of the XccFimX^{EAL}–c-di-GMP and SeMet-XccFimX^{EAL}–c-di-GMP–XccPilZ$_{1028}$ complexes. (a) XccFimX^{EAL}–c-di-GMP crystals grown in 0.2 M sodium formate pH 7.2, 20% PEG 3350 using the hanging-drop vapour-diffusion method at 277 K. These crystals reached average dimensions of 0.2 × 0.2 × 0.2 mm after one week. (b) SeMet-XccFimX^{EAL}–c-di-GMP–XccPilZ$_{1028}$ crystals grown in 0.1 M HEPES pH 7.5, 0.2 M NaCl, 20% PEG 3K using the hanging-drop vapour-diffusion method at 277 K. These crystals reached average dimensions of 0.01 × 0.01 × 0.01 mm after three weeks.
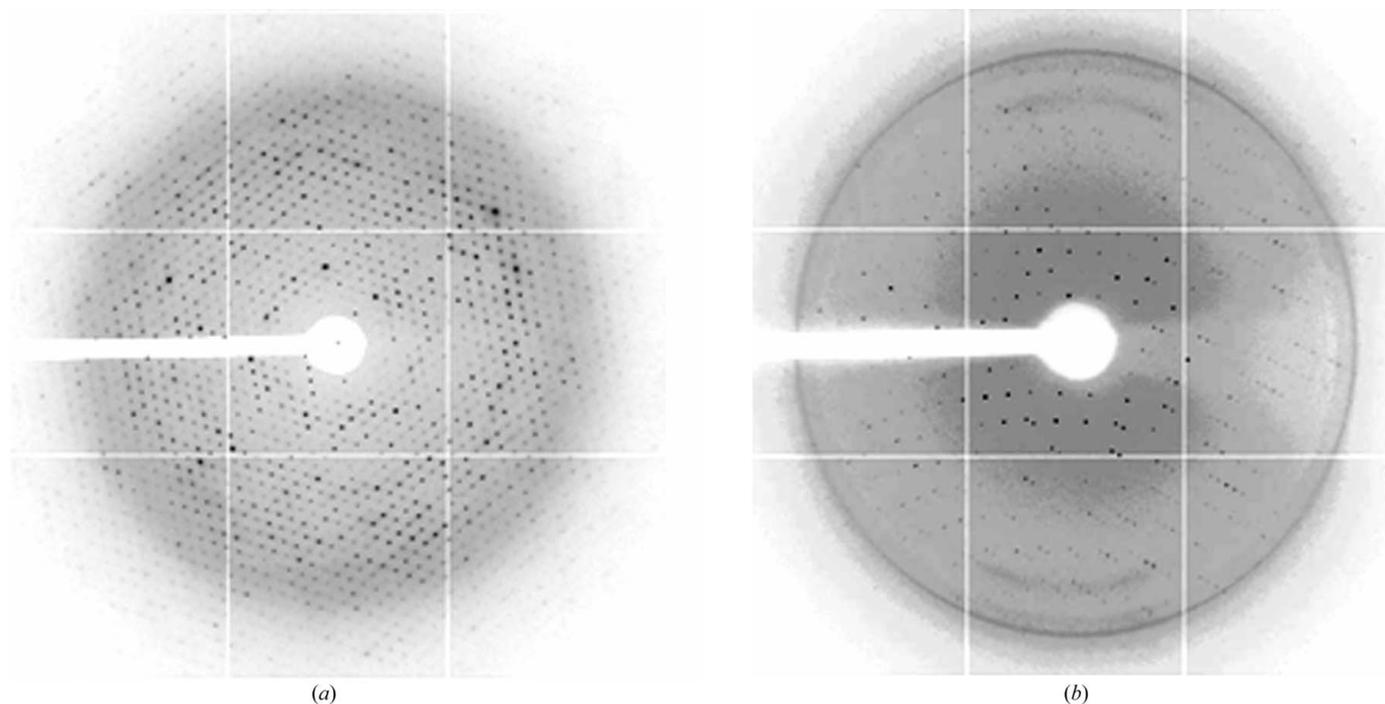
(a)   (b)

Figure 3
Diffraction patterns of the native XccFimX^{EAL}–c-di-GMP and SeMet-XccFimX^{EAL}–c-di-GMP–XccPilZ$_{1028}$ complexes collected on a MAR CCD system using synchrotron radiation on the 13B1 beamline at NSRRC in Taiwan and the BL12B1 beamline at SPring-8 in Japan. The exposure time was 1 s, the oscillation range was 1° per frame and the crystal-to-detector distance was 250 mm. The edge of the detector corresponds to a resolution of 2.5 and 3.2 Å, respectively.

to space group $P3_221$, while those of the XccFimX^{EAL}–c-di-GMP–XccPilZ$_{1028}$ complex belonged to space group $P6_322$. The diffraction statistics are summarized in Table 1.

3. Results and discussion

In this manuscript, we report the successful cloning, protein expression and purification of the XccFimX^{EAL} and XccPilZ$_{1028}$ proteins and the crystal screening and preliminary X-ray data analyses of the native XccFimX^{EAL}–c-di-GMP and SeMet-substituted XccFimX^{EAL}–c-di-GMP–XccPilZ$_{1028}$ complexes. Since the FimX protein is a large bacterial protein containing a tandem of REC, PAS, GGDEF and EAL domains, we tried to construct clones from different combinations of these domains as shown in Fig. 1(a) in order to express the domains and determine their structures using X-ray crystallography. Unfortunately, most of these constructs gave proteins in inclusion bodies and only XccFimX^{EAL} gave soluble protein. As shown in Fig. 1, the His$_6$ tag and linker of the XccFimX^{EAL} target could be successfully cleaved by TEV (tobacco etch virus) protease at 289 K for 10 h to obtain target protein that is more than 99% pure. It contains only an extra tripeptide (SNA) at the N-terminal end after further gel-filtration chromatography. However, in the absence of c-di-GMP no crystal formation was observed for the XccFimX^{EAL} domain and only a poor diffraction pattern was detected for the XccFimX^{EAL}–XccPilZ$_{1028}$ complex even though it formed seemingly good crystals. These results indicated that c-di-GMP was crucial in forming compact crystals for both the XccFimX^{EAL} domain and the XccFimX^{EAL}–XccPilZ$_{1028}$ complex.

We were surprised by the apparent existence of data to higher resolution once data collection for the native XccFimX^{EAL}-c-di-GMP complex began (Table 1) and are considering an experimental effort

to collect these data for refinement of the structure at higher resolution.

Interestingly, although the EAL-domain structure has been solved and found to be conserved (Minasov *et al.*, 2009; Navarro *et al.*, 2009; Tchigvintsev *et al.*, 2010), we were unable to solve the crystal structure of XccFimX^{EAL}–c-di-GMP using a molecular-replacement approach. Fortunately, we were able to crystallize the XccFimX^{EAL}–XccPilZ$_{1028}$ complex using an SeMet-substituted XccFimX^{EAL} domain in the presence of c-di-GMP. Although the resolution of the SeMet-XccFimX^{EAL}–c-di-GMP–XccPilZ$_{1028}$ complex was a little poorer (2.7 Å) than that of native XccFimX^{EAL}–c-di-GMP (2.5 Å), it should be possible to perform successful phasing of the protein using an Se-SAD approach based on the figure-of-merit statistic (Table 1). Indeed, the model of the XccFimX^{EAL} domain in the SeMet-XccFimX^{EAL}–c-di-GMP–XccPilZ$_{1028}$ complex was almost complete and the initial structure of XccFimX^{EAL} was used as a model for molecular replacement to determine the phases of the XccFimX^{EAL}–c-di-GMP complex. The Matthews coefficient and solvent content were 2.74 Å^3 Da^{-1} and 55.2%, respectively, for the XccFimX^{EAL}–c-di-GMP complex and 2.93 Å^3 Da^{-1} and 58.0%, respectively, for the SeMet-XccFimX^{EAL}–c-di-GMP–XccPilZ$_{1028}$ complex. The c-di-GMP was clearly identified in the electron-density maps of both the XccFimX^{EAL}–c-di-GMP and the SeMet-XccFimX^{EAL}–c-di-GMP–XccPilZ$_{1028}$ complexes. Refinement of both complexes is now in progress.

References

Alm, R. A., Bodero, A. J., Free, P. D. & Mattick, J. S. (1996). *J. Bacteriol.* **178**, 46–53.

Amikam, D. & Galperin, M. Y. (2006). *Bioinformatics*, **22**, 3–6.

Aslanidis, C. & de Jong, P. J. (1990). *Nucleic Acids Res.* **18**, 6069–6074.

Benach, J., Swaminathan, S. S., Tamayo, R., Handelman, S. K., Folta-Stogniew, E., Ramos, J. E., Forouhar, F., Neely, H., Seetharaman, J., Camilli, A. & Hunt, J. F. (2007). *EMBO J.* **26**, 5153–5166.

Brünger, A. T., Adams, P. D., Clore, G. M., DeLano, W. L., Gros, P., Grosse-Kunstleve, R. W., Jiang, J.-S., Kuszewski, J., Nilges, M., Pannu, N. S., Read, R. J., Rice, L. M., Simonson, T. & Warren, G. L. (1998). *Acta Cryst.* D**54**, 905–921.

Guzzo, C. R., Salinas, R. K., Andrade, M. O. & Farah, C. S. (2009). *J. Mol. Biol.* **393**, 846–866.

Huang, B., Whitchurch, C. B. & Mattick, J. S. (2003). *J. Bacteriol.* **185**, 7068–7076.

Jenal, U. & Malone, J. (2006). *Annu. Rev. Genet.* **40**, 385–407.

Kazmierczak, B. I., Lebron, M. B. & Murray, T. S. (2006). *Mol. Microbiol.* **60**, 1026–1043.

Li, T.-N., Chin, K.-H., Fung, K.-M., Yang, M.-T., Wang, A. H.-J. & Chou, S.-H. (2011). *PLoS One*, **6**, e22036.

Li, T.-N., Chin, K.-H., Liu, J.-H., Wang, A. H.-J. & Chou, S.-H. (2009). *Proteins*, **75**, 282–288.

Li, T.-N., Chin, K.-H., Shih, H.-L., Wang, A. H.-J. & Chou, S.-H. (2009). *Acta Cryst.* F**65**, 1056–1059.

Mattick, J. S. (2002). *Annu. Rev. Microbiol.* **56**, 289–314.

McCarthy, Y., Ryan, R. P., O'Donovan, K., He, Y.-Q., Jiang, B.-L., Feng, J.-X., Tang, J.-L. & Dow, J. M. (2008). *Mol. Plant Pathol.* **9**, 819–824.

Merighi, M., Lee, V. T., Hyodo, M., Hayakawa, Y. & Lory, S. (2007). *Mol. Microbiol.* **65**, 876–895.

Minasov, G., Padavattan, S., Shuvalova, L., Brunzelle, J. S., Miller, D. J., Baslé, A., Massa, C., Collart, F. R., Schirmer, T. & Anderson, W. F. (2009). *J. Biol. Chem.* **284**, 13174–13184.

Navarro, M. V., De, N., Bae, N., Wang, Q. & Sondermann, H. (2009). *Structure*, **17**, 1104–1116.

Otwinowski, Z. & Minor, W. (1997). *Methods Enzymol.* **276**, 307–326.

Pratt, J. T., Tamayo, R., Tischler, A. D. & Camilli, A. (2007). *J. Biol. Chem.* **282**, 12860–12870.

Qi, Y., Chuah, M. L.-C., Dong, X., Xie, K., Luo, Z., Tang, K. & Liang, Z.-X. (2011). *J. Biol. Chem.* **286**, 2910–2917.

Ramelot, T. A., Yee, A., Cort, J. R., Semesi, A., Arrowsmith, C. H. & Kennedy, M. A. (2007). *Proteins*, **66**, 266–271.

Rao, F., Pasunooti, S., Ng, Y., Zhuo, W., Lim, L., Liu, A. W. & Liang, Z.-X. (2009). *Anal. Biochem.* **389**, 138–142.

Römling, U. (2011). *Environ. Microbiol.*, doi:10.1111/j.1462-2920.2011.02617.x.

Römling, U. & Amikam, D. (2006). *Curr. Opin. Microbiol.* **9**, 218–228.

Römling, U., Gomelsky, M. & Galperin, M. Y. (2005). *Mol. Microbiol.* **57**, 629–639.

Ross, P., Mayer, R., Weinhouse, H., Amikam, D., Huggirat, Y., Benziman, M., de Vroom, E., Fidder, A., de Paus, P., Sliedregt, L. A. J. M., van der Marel, G. A. & van Boom, J. H. (1990). *J. Biol. Chem.* **265**, 18933–18943.

Ross, P., Weinhouse, H., Aloni, Y., Michaeli, D., Weinberger-Ohana, P., Mayer, R., Braun, S., de Vroom, E., van der Marel, G. A., van Boom, J. H. & Benziman, M. (1987). *Nature (London)*, **325**, 279–281.

Ryan, R. P., Fouhy, Y., Lucey, J. F., Crossman, L. C., Spiro, S., He, Y.-W., Zhang, L.-H., Heeb, S., Cámara, M., Williams, P. & Dow, J. M. (2006). *Proc. Natl Acad. Sci. USA*, **103**, 6712–6717.

Ryan, R. P., Fouhy, Y., Lucey, J. F., Jiang, B.-L., He, Y.-Q., Feng, J.-X., Tang, J.-L. & Dow, J. M. (2007). *Mol. Microbiol.* **63**, 429–442.

Ryjenkov, D. A., Simm, R., Römling, U. & Gomelsky, M. (2006). *J. Biol. Chem.* **281**, 30310–30314.

Simm, R., Morr, M., Kader, A., Nimtz, M. & Römling, U. (2004). *Mol. Microbiol.* **53**, 1123–1134.

Slater, H., Alvarez-Morales, A., Barber, C. E., Daniels, M. J. & Dow, J. M. (2000). *Mol. Microbiol.* **38**, 986–1003.

Stols, L., Gu, M., Dieckman, L., Raffen, R., Collart, F. R. & Donnelly, M. I. (2001). *Protein Expr. Purif.* **25**, 8–15.

Tal, R., Wong, H. C., Calhoon, R., Gelfand, D., Fear, A. L., Volman, G., Mayer, R., Ross, P., Amikam, D., Weinhouse, H., Cohen, A., Sapir, S., Ohana, P. & Benziman, M. (1988). *J. Bacteriol.* **180**, 4416–4425.

Tchigvintsev, A., Xu, X., Singer, A., Chang, C., Brown, G., Proudfoot, M., Cui, H., Flick, R., Anderson, W. F., Joachimiak, A., Galperin, M. Y., Savchenko, A. & Yakunin, A. F. (2010). *J. Mol. Biol.* **402**, 524–538.

Terwilliger, T. C. & Berendzen, J. (1999). *Acta Cryst.* D**55**, 849–861.

Tischler, A. D. & Camilli, A. (2004). *Mol. Microbiol.* **53**, 857–869.

Wu, Y.-Y., Chin, K.-H., Chou, C.-C., Lee, C.-C., Shr, H.-L., Gao, F. P., Lyu, P.-C., Wang, A. H.-J. & Chou, S.-H. (2005). *Acta Cryst.* F**61**, 902–905.